ADVANCED MATERIALS
www.advmat.de

Composition-Dependent Passivation Efficiency at the $CdS/CuIn_{1-x}Ga_xSe_2$ Interface

*Marco Ballabio, David Fuertes Marrón, Nicolas Barreau, Mischa Bonn, and Enrique Cánovas**

The bandgap of $CuIn_{1-x}Ga_xSe_2$ (CIGS) chalcopyrite semiconductors can be tuned between ≈1.0 and ≈1.7 eV for Ga contents ranging between $x = 0$ and $x = 1$. While an optimum bandgap of 1.34 eV is desirable for achieving maximum solar energy conversion in solar cells, state-of-the-art CIGS-based devices experience a drop in efficiency for Ga contents $x > 0.3$ (i.e., for bandgaps >1.2 eV), an aspect that is limiting the full potential of these devices. The mechanism underlying the limited performance as a function of CIGS composition has remained elusive: both surface and bulk recombination effects are proposed. Here, the disentanglement between surface and bulk effects in CIGS absorbers as a function of Ga content is achieved by comparing photogenerated charge carrier dynamics in air/CIGS and surface-passivated ZnO/CdS/CIGS samples. While surface passivation prevents surface recombination of charge carriers for low Ga content ($x < 0.3$; up to 1.2 eV bandgap), surface recombination dominates for higher-bandgap materials. The results thus demonstrate that surface, rather than bulk effects, is responsible for the drop in efficiency for Ga contents larger than $x \approx 0.3$.

Chalcopyrite semiconductors based on copper–indium–gallium–diselenide ($CuIn_{1-x}Ga_xSe_2$, CIGS) are currently commercially exploited as light-absorbers in thin-film solar cells.[1] CIGS alloys are an appealing choice for photovoltaics owing to their high absorption coefficient, as a result of their direct bandgap, enabling low-cost thin-film solar cells. In addition, CIGS absorbers can be grown onto flexible, light, and cheap substrates,[2] and have been reported to be more stable under prolonged sunlight irradiation when compared with other competing thin-film technologies such as those based on cadmium telluride (CdTe), amorphous silicon (a-Si), and novel perovskites.[3] A potential additional advantage of chalcopyrites is that the bandgap onset of $CuIn_{1-x}Ga_xSe_2$ quaternary alloys can be easily tuned by controlling the Ga content from ≈1.0 eV (gallium-free, $x = 0$, i.e., $CuInSe_2$) to ≈1.7 eV (indium-free, $x = 1$, i.e., $CuGaSe_2$). This feature allows for fine-tuning of the bandgap, which should enable a maximum theoretical photoconversion efficiency of 33.7% at an optimum bandgap of 1.34 eV (given by the Shockley–Queisser limit under an AM1.5 solar spectrum).[4,5] Remarkably, however, the record ≈23% efficiency of state-of-the-art of ZnO/CdS/CIGS solar cells employ CIGS absorbers with a bandgap of only ≈1.2 eV (Ga content of $x \approx 0.3$),[6,7] i.e., about 0.1 eV below the theoretical optimum.[8,9] This constraint results from the experimental observation that CIGS based solar cells employing Ga contents exceeding $x = 0.3$ undergo a significant reduction in photoconversion efficiency, which is largely driven by an increasing open-circuit-voltage deficit relative to the bandgap.[10]

The underlying reasons behind the experimentally observed output-voltage saturation of CIGS-based devices with a highGa content and its associated efficiency drop have been assigned in literature to different types of mechanisms which can be generally classified into bulk- or interface-limiting factors. Concerning bulk mechanisms, substantial differences in the energetics of point-defect formation of In- and Ga-containing species have been reported, with major penalties predicted for high Ga contents, that might lead to limitations on the maximum achievable splitting of quasi-Fermi levels (and the output voltage of the operating cells) and hampering type inversion of naturally occurring p-type material.[11,12] Additionally, bulk Ga-dependent trapping efficiency of minority carriers has been reported,[13,14] an aspect that might be contributed by a Ga-dependent diffusion efficiency into the bulk of elements like cadmium or sodium,[15,16] which are well-known grain boundary passivators.[17,18] Alternatively, theoretical works have predicted the promotion of metastable light-induced acceptors for high-Ga alloys,[19,20] which are

M. Ballabio, Prof. M. Bonn, Dr. E. Cánovas
Max Planck Institute for Polymer Research
Ackermannweg 10, 55128 Mainz, Germany
E-mail: enrique.canovas@imdea.org
Dr. D. Fuertes Marrón
Instituto de Energía Solar
Universidad Politécnica de Madrid
ETSI Telecomunicación
Avda. Complutense 30, 28040 Madrid, Spain
Dr. N. Barreau
Institut des Matériaux Jean Rouxel (IMN) – UMR6502
Université de Nantes
CNRS
2 rue de la Houssinière, BP 32229, 44322 Nantes Cedex 3, France
Dr. E. Cánovas
Instituto Madrileño de Estudios Avanzados en Nanociencia
(IMDEA Nanociencia)
Faraday 9, 28049 Madrid, Spain
The ORCID identification number(s) for the author(s) of this article can be found under https://doi.org/10.1002/adma.201907763.

DOI: 10.1002/adma.201907763

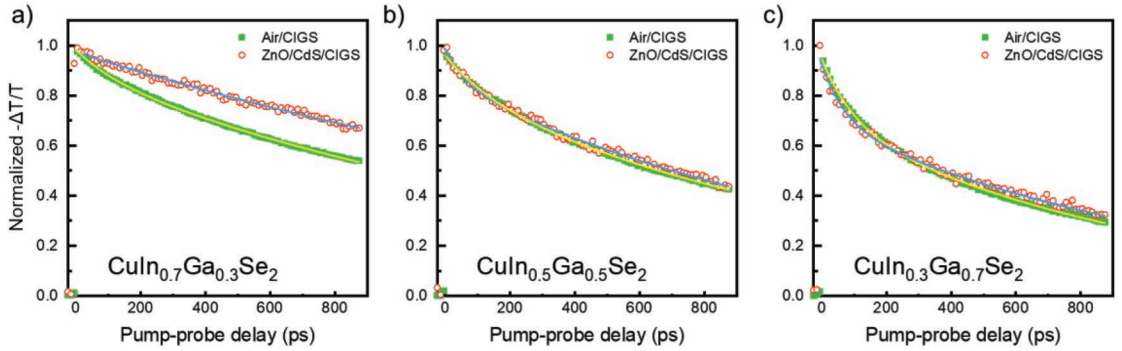

Figure 1. a–c) Normalized optical pump–THz probe dynamics on CIGS samples with Ga contents of $x = 0.3$ (a), $x = 0.5$ (b), and $x = 0.7$ (c). The green squares represent the decay for the air/CIGS samples, while the red open circles depict the transient signal for the ZnO/CdS/CIGS samples. The solid lines indicate the best biexponential fits to the data (single exponential for the low Ga ZnO/CdS/$CuIn_{0.7}Ga_{0.3}Se_2$ sample). In all cases, the photogenerated carrier density per pulse equals 1.7×10^{18} cm^{-3}.

expected to primarily populate the CIGS absorber close to the CdS junction (i.e., primarily a surface effect). Furthermore, Ga-dependent surface effects have been claimed to be responsible for the voltage deficit in state-of-the-art CdS/CIGS interfaces.[21] For example, the absence of an inversion layer at the interface between CIGS absorber and CdS buffer layer for bandgaps >1.2 eV,[7] or the transition from a barrier-like to a cliff-like conduction-band alignment with an increasing Ga content on the absorber side of the interface could explain the poor device performance of wide-gap-based CIGS devices.[22] Discriminating among these scenarios, therefore, requires disentangling surface from bulk effects on the carrier recombination processes in CIGS absorbers with different Ga contents, and their interplay with the CdS buffer layer.

In this work, we employ ultrafast photoconductivity measurements with sub-picosecond time resolution to investigate carrier dynamics in air/CIGS and device relevant ZnO/CdS/CIGS interfaces for a set of $CuIn_{1-x}Ga_xSe_2$ samples with Ga contents of $x = 0.3$, 0.5, and 0.7 (with bandgaps of ≈1.2, ≈1.3, and ≈1.5 eV, respectively). Our results demonstrate that while bulk charge dynamics are barely affected by the Ga content of CIGS alloys, surface recombination is stronger for higher Ga contents; this aspect is true for both air/CIGS and ZnO/CdS/CIGS interfaces. Notably, we also demonstrate that the CdS surface treatment of CIGS absorbers is only effective in inhibiting surface recombination for low-Ga-containing samples, having a negligible effect on samples with larger Ga contents (i.e., with $x = 0.5$ and 0.7). Finally, we resolve that interfacial recombination at the CdS/CIGS interface increases with photon flux for high-Ga samples, consistent with the formation of metastable acceptors at the interface. Our findings are in line with the observed Ga-dependent efficiency trend in device performance and demonstrate that its origin is linked to surface-, rather than bulk-assisted recombination.

Two-micrometer thick CIGS absorbers were deposited by coevaporation following a so-called isothermal three-stage process.[23] The Ga content of the layers (x) was tuned by adjusting Ga/In relative atomic fluxes from one deposition to another. Grown samples are denoted as $CuIn_{0.7}Ga_{0.3}Se_2$, $CuIn_{0.5}Ga_{0.5}Se_2$, and $CuIn_{0.3}Ga_{0.7}Se_2$; associated with a relative Ga content $x = \frac{[Ga]}{[Ga]+[In]}$ equal to 0.3, 0.5, and 0.7, respectively. The CIGS absorbers were deposited on both fused silica and standard Mo-coated soda-lime-glass substrate; the latter batch was used to fabricate complete solar cells; the solar efficiencies (η) were estimated to be 16.1%, 15.3%, and 11.7% for Ga contents of $x = 0.3$, 0.5, and 0.7, respectively (see the Supporting Information). Up to six samples were deposited onto fused 1 mm thick silica substrates; three of them remained uncovered (air/CIGS samples) and three of them were covered by a 50 nm CdS buffer layer applied by chemical bath deposition and 50 nm ZnO by RF-sputtering from a ceramic target (samples denoted as ZnO/CdS/CIGS).

We performed optical pump–terahertz probe (OPTP) experiments on the six samples consisting of air/CIGS and ZnO/CdS/CIGS structures with three different Ga contents.[24,25] For materials in which the photoexcited layer (l), chosen to be equal to the light penetration depth, is sufficiently thin compared to the sample thickness, it is possible to obtain the photoconductivity of the samples by deriving the following analytic formula that links the measurable THz differential transmission $\left(\frac{\Delta T}{T^{ref}}\right)$ with the transient photoconductivity ($\Delta\sigma$)[26,27]

$$\Delta\sigma = -\frac{n_1 + n_2}{Z_0 \cdot l} \cdot \frac{\Delta T}{T^{ref}} \quad (1)$$

where $n_{1,2}$ are respectively the refractive indexes, in the THz range, of the medium before and after the photoexcited region, and Z_0 is the free space impedance. In our experiments, the pump light penetration depth at 800 nm was inferred to be 177, 220, and 340 nm for $CuIn_{0.7}Ga_{0.3}Se_2$, $CuIn_{0.5}Ga_{0.5}Se_2$, and $CuIn_{0.3}Ga_{0.7}Se_2$, respectively, based on the data published by Paulson et al.[28] For all the measurements conducted in this study, we observe a linear correlation between the photon flux and the maximum transient transmittance, demonstrating that the carrier dynamics are probed in the linear regime, and that the carrier mobility is independent of carrier density. The efficiency of photogeneration right after light pump excitation is resolved to be unity for all samples (see Figure S1, Supporting Information).

Figure 1 presents three panels comparing normalized TRTS dynamics for air/CIGS (green traces) and ZnO/CdS/CIGS samples (red traces), as defined by the three analyzed Ga contents. The pump photons (800 nm wavelength and pulse duration

of 45 fs at 1 kHz repetition rate), impinging on the samples from either the air or the ZnO/CdS window, selectively excite the CIGS layer (i.e., the excitation wavelength is unable to produce direct band-to-band transitions in ZnO/CdS capping materials). The light intensity was adjusted according to the penetration depth in order to have the same photogenerated carrier density in all the samples ($\approx 1.7 \times 10^{18}$ cm^{-3}). As follows from Equation (1), $\frac{\Delta T}{T^{\text{ref}}}$ is directly proportional to the sample's photoconductivity $\Delta\sigma = e\Delta N\Delta\mu$ (where e is the electron charge, ΔN is the photoinduced charge carrier density, and $\Delta\mu$ is the photoinduced electrical mobility), the resolved dynamics in Figure 1 might—in principle—reveal photoinduced changes in both carrier density and/or mobility as a function of time. Analysis of the THz frequency-resolved complex conductivity (see the Supporting Information) as a function of pump–probe delay demonstrates that mobility is barely affected upon pump–probe delay for each set of samples (i.e., $\Delta\mu(t) = \mu$). As such, the monitored dynamics in each panel of Figure 1 are primarily revealing recombination kinetics in the samples (that is, $\Delta\sigma(t) = e\Delta N(t)\mu$). Provided that the electron effective mass is between 2 and 4 times lighter than the hole effective mass for Ga contents between 0 and 1,[29] we interpret our OPTP signal as describing predominantly electron dynamics.

First, we compare the electron recombination kinetics for samples consisting of air/$CuIn_{1-x}Ga_xSe_2$ interfaces (green squares) as a function of Ga content. As evident from the plots in Figure 1, the electron dynamics for air/CIGS samples can be well described by a biexponential function with fast and slow decay time constants of $\tau_{\text{fast}} \approx 100$ ps and $\tau_{\text{slow}} \approx 1000$ ps (the origin for this biexponential deactivation path is discussed later). As the Ga content is increased, the overall recombination kinetics becomes faster (see green traces in Figure 1a–c). This result alone demonstrates that increasing Ga contents leads to enhanced recombination rates in the CIGS layers.

Interestingly, comparing air/CIGS kinetics with those obtained from ZnO/CdS/$CuIn_{1-x}Ga_xSe_2$ samples with high Ga contents ($x = 0.5$ and 0.7; red symbols in Figure 1b,c), reveals that charge carrier dynamics are barely affected by the presence of ZnO/CdS overlayers. That is, ZnO/CdS capping does not induce any measurable passivating effect on samples with bandgaps above 1.2 eV. This result demonstrates a negligible effect of the CdS buffer layer on inhibiting surface (or bulk) recombination in samples with a high Ga content. On the other hand, the sample with the lower Ga content ($x = 0.3$ and bandgap of ≈1.2 eV, the state-of-the-art composition), shows a clear change in recombination kinetics upon CdS treatment. The CdS treatment produces a 24% increase in amplitude at 900 ps after pump excitation that demonstrates unambiguously an improvement in carrier density (photocurrent) resulting from effective passivation of the CdS/CIGS interface. Notably, the CdS capping gives rise to the disappearance of the fast decay component, leaving the dynamics single-exponential, defined only by the ≈1000 ps long-lived τ_{slow} component, also observed for the uncapped samples. Therefore, we can conclude that the fast component τ_{fast} is associated with trapping at the CdS/CIGS interface (i.e., with interfacial recombination). Overall, the results shown in Figure 1 demonstrate that the passivating effect of the CdS treatment onto CIGS absorbers is Ga-dependent; being uniquely effective for the low Ga content sample. These observations correlate very well with the drop in efficiency observed in CIGS-based devices with high Ga contents ($x > 0.3$; for solar cells obtained from these samples see Table S1 in the Supporting Information). In addition, OPTP dynamics for samples deposited onto soda-lime glass and fused silica are indistinguishable (see the Supporting Information), revealing that the nature of the substrate employed in THz measurements and solar cell devices does not substantially alter the chemistry of the samples at the probed interface.

To validate the conclusion that the surface recombination component is uniquely associated with the fast ≈100 ps component, we performed a fluence-dependent analysis of the samples. The intention was to deliberately saturate surface traps by photodoping. **Figure 2**a presents optical pump–THz probe traces as a function of incident photon density for the low-Ga sample exposed to air within the range of 3.0×10^{12} to 2.2×10^{14} photons cm^{-2} per pulse (with estimated carrier densities in the range between 1.7×10^{17} and 1.2×10^{19} cm^{-3}, comparable with solar cell devices operating under 1 sun illumination, see the Supporting Information). As it is evident from the plot, increasing the pump fluence for the low-Ga air/CIGS sample results in a reduction of the weight of the fast recombination component. For sufficiently high photon fluxes, the dynamics become single exponential and defined only by the long-lived ≈1000 ps component. The lifetimes and relative amplitudes obtained from biexponential fits to the data for the evolution of the fast and slow kinetic components as a function of photon flux are summarized in Figure 2b,c. The data reveal that τ_{slow} (linked to CIGS bulk recombination) is barely affected by fluence over the analyzed range of excitations. However, τ_{fast} (linked to surface recombination at the air/CIGS interface) becomes smaller in amplitude and that at elevated photon fluxes, increasingly slower trapping timescales are obtained (consistent with the notion that that trapping rate is directly proportional to trap density).[30–32] Also, we observe that the carrier dynamics of the low Ga content for ZnO/CdS/CIGS samples at low fluences (open green dots in Figure 2a) correlate very well with those obtained for air/CIGS samples at high photon fluences, suggesting that photodoping reaches almost the same passivating effect as the CdS-capping. These observations confirm the assignment of the fast and slow trapping components to surface and bulk effects, respectively.

Finally, we performed fluence-dependent analysis for the high-Ga samples ($x = 0.5$ and $x = 0.7$ Ga contents, bare data can be found in the Supporting Information). Quantitative analysis of the data, from biexponential fits (see **Figure 3**a,b), reveal, when compared with the low-Ga sample (Figure 2c), a much weaker trap filling effect (affecting only the fast surface-related component) for the sample with Ga content of $x = 0.5$. On the other hand, no evidence is found for trap filling in the high-Ga sample ($x = 0.7$, Figure 3b), which presents almost invariant trapping time constants of ≈100 and ≈1000 ps for all the analyzed photon fluences corresponding to carrier densities ranging from $\approx 10^{17}$ to 10^{19} cm^{-3}. These results illustrate that the surface defect population for high-Ga samples is much larger than the maximum carrier density induced by the larger photon flux employed in this study ($\approx 10^{19}$ cm^{-3}). The relative amplitudes for the slow and fast components obtained from

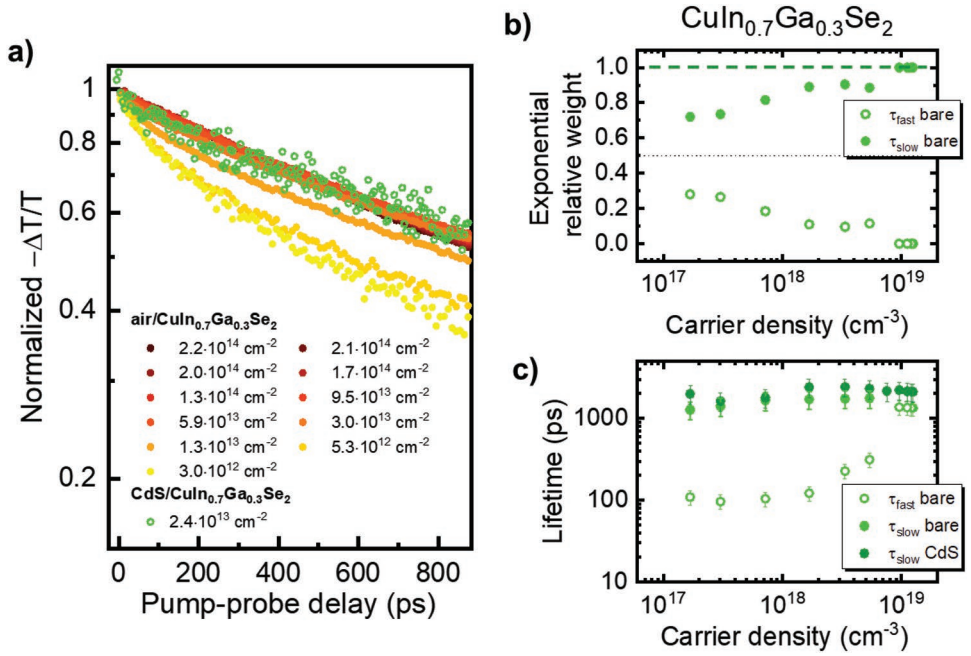

Figure 2. a) Comparison between charge dynamics in air/$CuIn_{0.7}Ga_{0.3}Se_2$ with increasing excitation density (solid dots) and CdS/$CuIn_{0.7}Ga_{0.3}Se_2$ (green open circles). b,c) The relative weight and lifetimes obtained from biexponential fits to the data as a function of photoinduced carrier density.

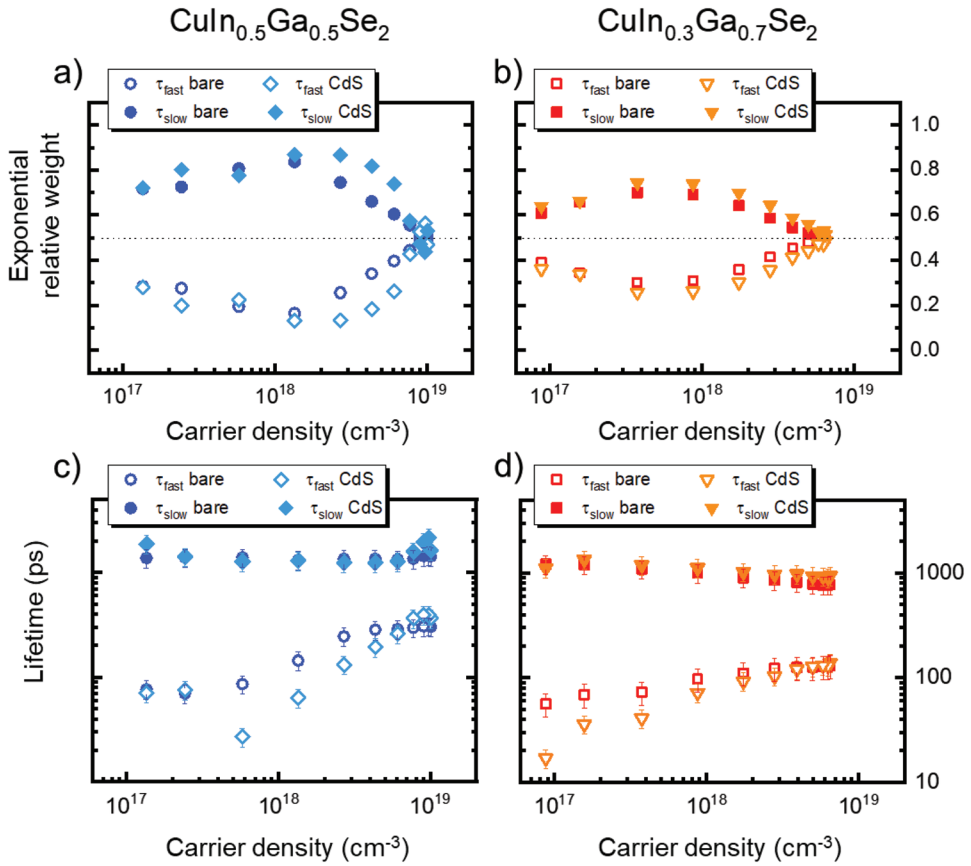

Figure 3. a,b) Relative weight of the time constants as a function of the charge carriers photogenerated in the system according to the biexponential fit for $CuIn_{0.5}Ga_{0.5}Se_2$ (a) and $CuIn_{0.3}Ga_{0.7}Se_2$ (b). c,d) The respective lifetime extracted for the two samples.

biexponential fits to the data are presented in Figure 3c,d. Notably, the data reveal that, at elevated charge densities, both high Ga content samples ($x = 0.5$ and $x = 0.7$) show an increase in the weight associated with the component ascribed to surface recombination, suggesting an increase in defect population at the CdS/CIGS interface with photon flux. We interpret this observation with the promotion of metastable light-induced acceptors for high-Ga alloys.[19,20] These metastable traps have been associated with the formation of divacancies (V_{Se}–V_{Cu}) at the CdS/CIGS interfaces under "red illumination" (i.e., light not absorbed by the window/buffer layer as in our experimental conditions) and are expected to be dominant for high Ga content CIGS absorbers. The Ga content-dependent promotion of interfacial traps induced by light at the CdS/CIGS surface underlines even more the main conclusion of this paper: Ga-dependent surface recombination—rather than bulk—determines photoconversion efficiency in CIGS samples as a function of Ga content.

In conclusion, we report the interplay between surface recombination and CIGS stoichiometry. We demonstrate that surface recombination is Ga content-dependent for CIGS absorbers, at both air/CIGS and ZnO/CdS/CIGS interfaces; being increasingly dominant for samples with larger Ga contents and therefore larger bandgaps. Furthermore, we demonstrate that CdS capping is only effective in removing surface recombination for the low-Ga samples. Our data further reveal the formation of light-induced acceptors at the CdS/CIGS interface for high-Ga samples. Altogether, our results correlate well with the observed Ga-dependent efficiency trend in device performance and demonstrate that the drop of efficiency in cells made with larger bandgaps can be attributed, at least partially, to surface—rather than bulk—recombination at the CdS/CIGS interface. Note that the relative band alignment at the CdS/CIGS interface as a function of Ga content might impose as well a V_{oc} deficit in solar cells. Interfacial engineering could, therefore, prove a way forward for further increasing the efficiency of CdS/CIGS-based devices.[33]

Supporting Information

Supporting Information is available from the Wiley Online Library or from the author.

Acknowledgements

D.F.M. acknowledges financial support from Ministerio de Ciencia, Innovación y Universidades, ENE2017-89561-C4-2-R. E.C. acknowledges financial support from the Max Planck Society, the regional government of Comunidad de Madrid (2017-T1/AMB-5207) and the "Severo Ochoa" Programme for Centres of Excellence in R&D (MINECO, Grant No. SEV-2016-0686). The authors acknowledge the collection of preliminary TRTS data on CIGS samples conducted by Dr. Hai Wang and Dr. Soeren Jensen.

Conflict of Interest

The authors declare no conflict of interest.

Keywords

CIGS, CIGS/CdS, interfacial recombination, solar cells, THz spectroscopy

Received: November 26, 2019
Revised: December 24, 2019
Published online: January 27, 2020

[1] M. A. Green, E. D. Dunlop, D. H. Levi, J. Hohl-Ebinger, M. Yoshita, A. W. Y. Ho-Baillie, *Prog. Photovoltaics Res. Appl.* **2019**, *27*, 565.
[2] A. Chirilă, S. Buecheler, F. Pianezzi, P. Bloesch, C. Gretener, A. R. Uhl, C. Fella, L. Kranz, J. Perrenoud, S. Seyrling, R. Verma, S. Nishiwaki, Y. E. Romanyuk, G. Bilger, A. N. Tiwari, *Nat. Mater.* **2011**, *10*, 857.
[3] J. F. Guillemoles, L. Kronik, D. Cahen, U. Rau, A. Jasenek, H. W. Schock, *J. Phys. Chem. B* **2000**, *104*, 4849.
[4] W. Shockley, H. J. Queisser, *J. Appl. Phys.* **1961**, *32*, 510.
[5] S. Rühle, *Sol. Energy* **2016**, *130*, 139.
[6] M. A. Green, Y. Hishikawa, E. D. Dunlop, D. H. Levi, J. Hohl-Ebinger, M. Yoshita, A. W. Y. Ho-Baillie, *Prog. Photovoltaics Res. Appl.* **2019**, *27*, 3.
[7] R. Herberholz, V. Nadenau, U. Rühle, C. Köble, H. W. Schock, B. Dimmler, *Sol. Energy Mater. Sol. Cells* **1997**, *49*, 227.
[8] W. N. Shafarman, R. Klenk, B. E. Mccandless, *J. Appl. Phys.* **1996**, *79*, 7324.
[9] A. Yamada, K. Matsubara, K. Sakurai, S. Ishizuka, H. Tampo, P. J. Fons, K. Iwata, S. Niki, *Appl. Phys. Lett.* **2004**, *85*, 5607.
[10] P. K. Nayak, S. Mahesh, H. J. Snaith, D. Cahen, *Nat. Rev. Mater.* **2019**, *4*, 269.
[11] Y.-J. Zhao, C. Persson, S. Lany, A. Zunger, *Appl. Phys. Lett.* **2004**, *85*, 5860.
[12] S. B. Zhang, S.-H. Wei, A. Zunger, H. Katayama-Yoshida, *Phys. Rev. B* **1998**, *57*, 9642.
[13] G. Hanna, A. Jasenek, U. Rau, H. W. Schock, *Thin Solid Films* **2001**, *387*, 71.
[14] J. T. Heath, J. D. Cohen, W. N. Shafarman, D. X. Liao, A. A. Rockett, *Appl. Phys. Lett.* **2002**, *80*, 4540.
[15] S. Shirakata, K. Ohkubo, Y. Ishii, T. Nakada, *Sol. Energy Mater. Sol. Cells* **2009**, *93*, 988.
[16] D. Rudmann, G. Bilger, M. Kaelin, F.-J. Haug, H. Zogg, A. N. Tiwari, *Thin Solid Films* **2003**, *431*, 37.
[17] L. Kronik, D. Cahen, H. W. Schock, *Adv. Mater.* **1998**, *10*, 31.
[18] D. W. Niles, M. Al-Jassim, K. Ramanathan, *J. Vac. Sci. Technol., A* **1999**, *17*, 291.
[19] S. Lany, A. Zunger, *J. Appl. Phys.* **2006**, *100*, 113725.
[20] J.-F. Guillemoles, L. Kronik, D. Cahen, U. Rau, A. Jasenek, H.-W. Schock, *J. Phys. Chem. B* **2000**, *104*, 4849.
[21] T. Minemoto, T. Matsui, H. Takakura, Y. Hamakawa, T. Negami, Y. Hashimoto, T. Uenoyama, M. Kitagawa, *Sol. Energy Mater. Sol. Cells* **2001**, *67*, 83.
[22] R. Klenk, *Thin Solid Films* **2001**, *387*, 135.
[23] F. Couzinié-Devy, N. Barreau, J. Kessler, *Prog. Photovoltaics Res. Appl.* **2011**, *19*, 527.
[24] R. Ulbricht, E. Hendry, J. Shan, T. F. Heinz, M. Bonn, *Rev. Mod. Phys.* **2011**, *83*, 543.
[25] H. Němec, P. Ňuel, V. Sundström, *J. Photochem. Photobiol., A* **2010**, *215*, 123.
[26] P. Kužel, F. Kadlec, H. Němec, *J. Chem. Phys.* **2007**, *127*, 24506.
[27] P. U. Jepsen, D. G. Cooke, M. Koch, *Laser Photonics Rev.* **2011**, *5*, 124.

[28] P. D. Paulson, R. W. Birkmire, W. N. Shafarman, *J. Appl. Phys.* **2003**, *94*, 879.
[29] R. Chen, C. Persson, *Thin Solid Films* **2011**, *519*, 7503.
[30] M. Lambsdorff, J. Kuhl, J. Rosenzweig, A. Axmann, J. Schneider, *Appl. Phys. Lett.* **1991**, *58*, 1881.
[31] H. Wang, I. Barceló, T. Lana-Villarreal, R. Gómez, M. Bonn, E. Cánovas, *Nano Lett.* **2014**, *14*, 5780.
[32] F. E. Doany, D. Grischkowsky, C.-C. Chi, *Appl. Phys. Lett.* **1987**, *50*, 460.
[33] W. Jaegermann, A. Klein, T. Mayer, *Adv. Mater.* **2009**, *21*, 4196.